van der Waals Heterostructure of Phosphorene and Graphene: Tuning the Schottky Barrier and Doping by Electrostatic Gating

J. E. Padilha,[1,*] A. Fazzio,[1,†] and Antônio J. R. da Silva[1,2,‡]
[1]*Instituto de Física, Universidade de São Paulo, CP 66318, 05315-970, São Paulo, SP, Brazil*
[2]*Laboratório Nacional de Luz Síncrotron, CP 6192, 13083-970, Campinas, SP, Brazil*
(Received 23 October 2014; published 12 February 2015)

In this Letter, we study the structural and electronic properties of single-layer and bilayer phosphorene with graphene. We show that both the properties of graphene and phosphorene are preserved in the composed heterostructure. We also show that via the application of a perpendicular electric field, it is possible to tune the position of the band structure of phosphorene with respect to that of graphene. This leads to control of the Schottky barrier height and doping of phosphorene, which are important features in the design of new devices based on van der Waals heterostructures.

DOI: 10.1103/PhysRevLett.114.066803 PACS numbers: 73.22.Pr, 73.30.+y, 74.25.N-, 74.78.Fk

Two-dimensional (2D) materials have been considered key ingredients for the future of nanoelectronics and optoelectronics. Besides their exquisite properties, they have the potential to lead to drastic reductions in the characteristic lengths of devices [1–3]. The very first material that boosted the research area in 2D materials was graphene [4,5]. Graphene, a hexagonal lattice of carbon atoms, has been considered since its isolation one of the promising candidates for future applications in nanoscale electronics [6,7]. However, the absence of either an electronic band gap or a controllable way to create this gap without destroying graphene's significant properties has limited its applications [6]. Subsequently to the graphene isolation, a whole new class of 2D materials has been studied [2,3,8], such as the transition metal dichalchogenides [9,10].

Very recently, phosphorene, a single layer of phosphorus arranged in a hexagonal puckered lattice, was isolated from the bulk black phosphorus structure [11–13]. In this case, bulk black phosphorus is the graphite counterpart of phosphorene, where the phosphorene layers are bonded together through van der Waals interactions. This rediscovered material presents very interesting properties provided by its unique band structure, including its highly anisotropic effective masses and electronic properties that can be tuned by strain, creating a sequence of transitions like direct semiconductor, indirect semiconductor, semimetal, and metal [14,15]. Also, this new elemental material presents a high electron mobility ($\approx$1000 $cm^2/V \cdot s$) [13] and a transport band gap that changes considerably as a function of the number of layers, going from 0.3 eV for the bulk black phosphorus to around 2 eV for a monolayer. All these properties make this material important for applications in both nanoelectronics and optoelectronics [11,16–18].

Currently, vertical heterostructures based on 2D van der Waals materials are being considered as a novel way to construct devices that integrate the properties of their isolated components [1,19,20] with ideal properties to be applied in nanoelectronics [21–23] and optoelectronics [9,24,25]. This layer-by-layer assembly is only possible due to the lack of dangling bonds in the 2D materials, in such a way that when two or more different materials are bonded together, their properties are preserved without any degradation. For example, recently a truly two-dimensional nanotransistor has been constructed using heterostructures of graphene, MoS_2, and hexagonal boron nitride, where graphene acts as both source or drain and gate electrodes, *h–BN* as the high-*k* dielectric, and MoS_2 as the channel [26].

In this new paradigm of van der Waals layer-by-layer epitaxy, researchers are starting to use graphene as the contact in a device rather than the channel. This approach has been successfully applied in several systems [21,26,27]. Thus, the same approach can be used to construct a system based on phosphorene, without the necessity to use a metal surface as the contact since, as already demonstrated by Gong *et al.* [28], the phosphorene layer strongly binds to the metal surface, degrading its properties.

In this Letter, we study the structural and electronic properties of single-layer and bilayer phosphorene stacked on top of graphene. We show that both the properties of graphene and phosphorene are preserved upon their contact. Moreover, we also show that it is possible to tune the position of the band structure of phosphorene with respect to that of graphene through the application of an external electrical field perpendicular to the system. This allows the control of the Schottky barrier height and the doping level of phosphorene, which is essential in the design of new devices based on this kind of layered structure.

To study the structural and electronic properties of single-layer and bilayer phosphorene contacted with graphene, we used state-of-the-art *ab initio* simulations, based on the density functional theory (DFT) as implemented in the VASP code [29,30]. We used the generalized gradient

approximation for the exchange and correlation potential, as proposed by Perdew-Burk-Ernzerhof (PBE) [31], the projector augmented wave potential (PAW) [32] to treat the ion-electron interactions, and a plane-wave cutoff energy of 500 eV. To correctly describe the effect of a van der Waals interaction, we employed a dispersion-corrected DFT method (optB88-vdW) [33,34], which has been demonstrated to reliably describe phosphorene systems [35–37]. With the optimized structures, the HSE06 hybrid functional [38,39] was used to calculate the band structures of the systems [40]. The band structures, work functions, and band edges were aligned with respect to the vacuum level, obtained via the electrostatic potentials of the systems.

In Fig. 1(a) [Fig. 1(b)], we show the structure of a single layer [bilayer] of phosphorene on top of graphene. The unit cell of our system is composed by 1×4 unit cells of graphene and 1×3 unit cells of phosphorene along the x and y directions. All structures were relaxed (lattice constant and atomic positions) until the residual forces on the atoms were smaller than 0.001 eV/Å. As the phosphorene properties are very sensitive to any strain condition [14], to compensate the lattice mismatch between phosphorene and graphene, we chose to keep the phosphorene lattice fixed, and stretched the graphene system.

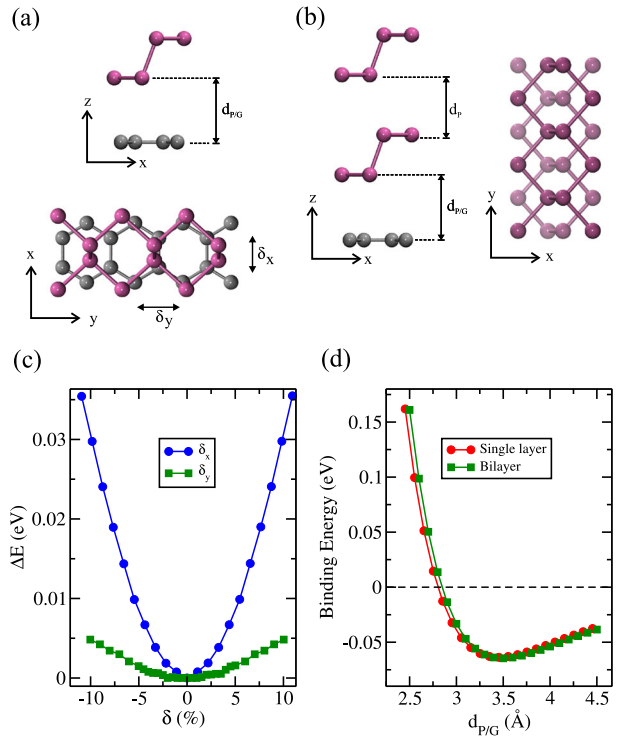

FIG. 1 (color online). (a) Side and top view of a single layer of phosphorene on top of graphene. (b) Side and top view of a bilayer of phosphorene on top of graphene. (c) Evolution of the total energy as a function of displacements $\delta_{x/y}$ of the phosphorene layer relative to graphene, taking the origin at the lowest energy configuration. (d) Binding energy as a function of the distance $d_{P/G}$, for the single-layer and bilayer system.

The overall induced strain in the graphene lattice is around 1%, and no significant changes were observed in its electronic structure. The configuration depicted in Fig. 1(a) is the equilibrium geometry of the system. To obtain this configuration, we relaxed the composed structure using several starting positions of the phosphorene layer relative to the graphene one. From the lowest energy configuration we have found, we moved the phosphorene layer with respect to the graphene layer by finite amounts $\delta_{x/y}$, in order to make sure this was really the minimum energy configuration. Depicted in Fig. 1(c) is the evolution of the total energy difference as a function of $\delta_{x/y}$. As can be seen, the minimum along the x direction is more pronounced than along the y direction [The same behavior was also observed for the bilayer system, not shown in Fig. 1(c)]. Moreover, since the energy differences for the distinct displacements are quite small, there might be the possibility that the phosphorene layer stays trapped in a position distinct from the lowest energy one due to the growth process. We thus calculated the electronic structure for several displacements δ_x and δ_y and in comparison with the equilibrium position; no significant changes were observed in the electronic structure (see the Supplemental Material, Fig. S1 [44]). We also calculated the electronic structure of the single-layer phosphorene on top of graphene, fixing the lattice of the system to the graphene layer (see the Supplemental Material, Fig. S2 [44]). Even though the properties of phosphorene are more sensitive to strain than those of graphene, the main results do not change.

Given the equilibrium position of the phosphorene system with respect to the graphene layer, we calculated the binding energy, per carbon atom, between the graphene sheet and the single-layer and bilayer phosphorene $\{E_b = [E_{P(BP)/G} - (E_{P(BP)} + E_G)]/N\}$, where $E_{P(BP)/G}$ is the total energy of the single layer (P) [bilayer (BP)] phosphorene plus graphene (G) heterostructure, $E_{P(BP)}$ is the total energy of the isolated single layer (P) [bilayer (BP)] phosphorene, E_G is the total energy of the isolated graphene layer, and $N_C = 16$ is the number of carbon atoms in the unit cell. For the single-layer phosphorene, the binding energy is about 60 meV with an equilibrium distance of 3.45 Å. For the bilayer, the binding energy is virtually the same as for the single layer, whereas the equilibrium distance is 3.49 Å. Those binding energies have the same order of magnitude as other van der Waals crystals, such as bilayer graphene [$E_b(BG) = 50$ meV = our calculation], graphite ($E_b = 61$ meV), and bulk hexagonal boron nitride [$E_b(h-BN) = 65$ meV] [45].

In Fig. 2, we show the projected band structure for the single-layer and bilayer phosphorene on top of graphene. We show in (a) [(c)] the contribution of the phosphorous atoms and in (b) [d] the contribution of the carbon atoms for the single-layer [bilayer] phosphorene system. As can be seen, the electronic structure of both the phosphorene and the graphene layers are quite well preserved upon binding. This result is significant because it shows that all properties

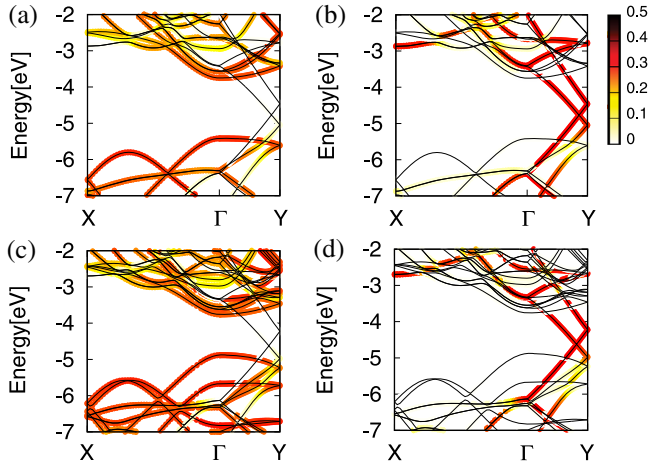

FIG. 2 (color online). Band structure of single-layer phosphorene on top of graphene projected at the (a) phosphorene layer and (b) graphene layer. Band structure of bilayer phosphorene on top of graphene projected at the (c) bilayer phosphorene and (d) graphene layer. The scale indicates the magnitude of the projection.

of the isolated materials are conserved, an important behavior for 2D van der Waals heterostructures

In Fig. 3, we make a comparison between the band structures of (a) the single-layer phosphorene with graphene with the (b) pristine single-layer phosphorene, and between those of (d) bilayer phosphorene with graphene with (e) pristine bilayer phosphorene. No significant changes are observed between the composed and the pristine systems, as mentioned above. However, a close inspection shows that the weak interaction between phosphorene and graphene results in a band gap increase of 0.1 eV for the single-layer and 0.05 eV for the bilayer phosphorene, as shown in Fig. 3(c) and 3(f), respectively. The band gap is 1.64 eV (1.51 eV without graphene) for the single-layer and 1.09 eV (1.04 eV without graphene) for the bilayer phosphorene, where the increase of these band gaps results solely from the interaction between the pz orbitals of the phosphorene with the π cloud of graphene.

Even without any charge transfer between the phosphorene systems and graphene, if we think of an in-plane current device, there will be a small band bending as one moves from the region where there are stacked phosphorene and graphene layers to the region where only the pristine phosphorene is present. We can estimate this band bending by the difference between the Fermi levels of the phosphorene with graphene system and the free-standing phosphorene [46]: $\Delta E_F = W - W_P$, where W is the work function of the composed system (phosphorene or graphene) and W_P is the work function of the pristine phosphorene. From the results shown in Fig. 3(c) for the single layer and (f) for the bilayer, we estimate that this band bending is 0.15 eV for the single-layer and 0.17 eV for the bilayer phosphorene. As $\Delta E_F > 0$ for both systems, electrons will be transferred from the noncontacted phosphorene region to the phosphorene and graphene one, making the channel p-type. These results are opposite those obtained by *ab initio* calculations of phosphorene on conventional metals, which predict a n-type contact [28].

From a device point of view, when using graphene as the metal contact and the single-layer or bilayer phosphorene as the channel, it is very important to know its Schottky barrier height (SBH). For these systems, we can define the SBH via the Schottky-Mott rule, since there is no chemical bond between the layers and also there is no charge transfer

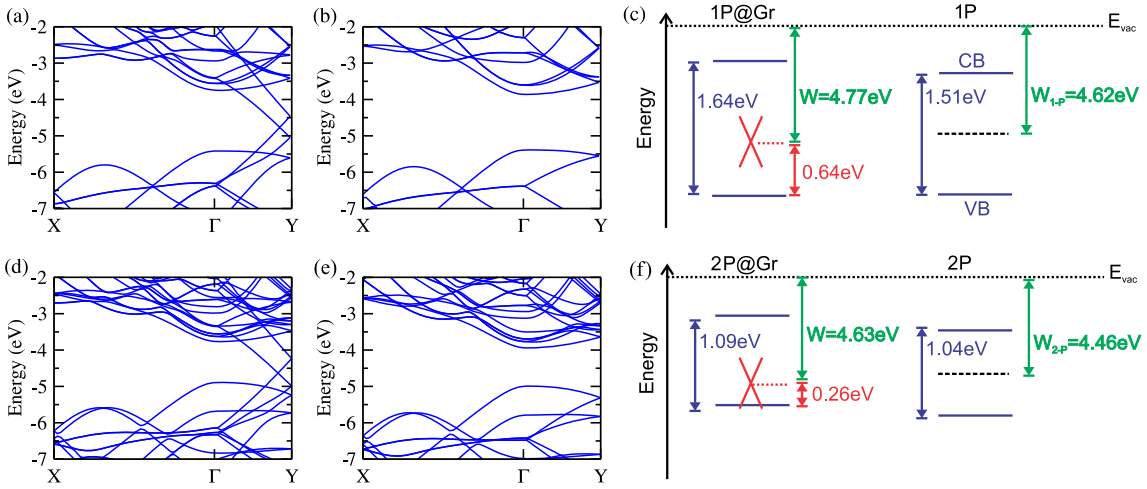

FIG. 3 (color online). (a) Band structure of single-layer phosphorene with graphene (1P@Gr), (b) band structure of single-layer phosphorene (1P) without graphene, and (c) band edges of the (left panel) composed system and (right panel) pristine single-layer phosphorene. (d) Band structure of bilayer phosphorene with graphene (2P@Gr), (e) band structure of bilayer phosphorene (2P) without graphene, and (f) band edges of the (left panel) composed system and (right panel) pristine bilayer phosphorene. The horizontal blue lines in (c) and (f) represent the valence band (VB) and conduction band (CB) of phosphorene. The red crossed lines represent the Dirac cone of graphene and W is the work function. All values presented in this figure were aligned with respect to the vacuum level.

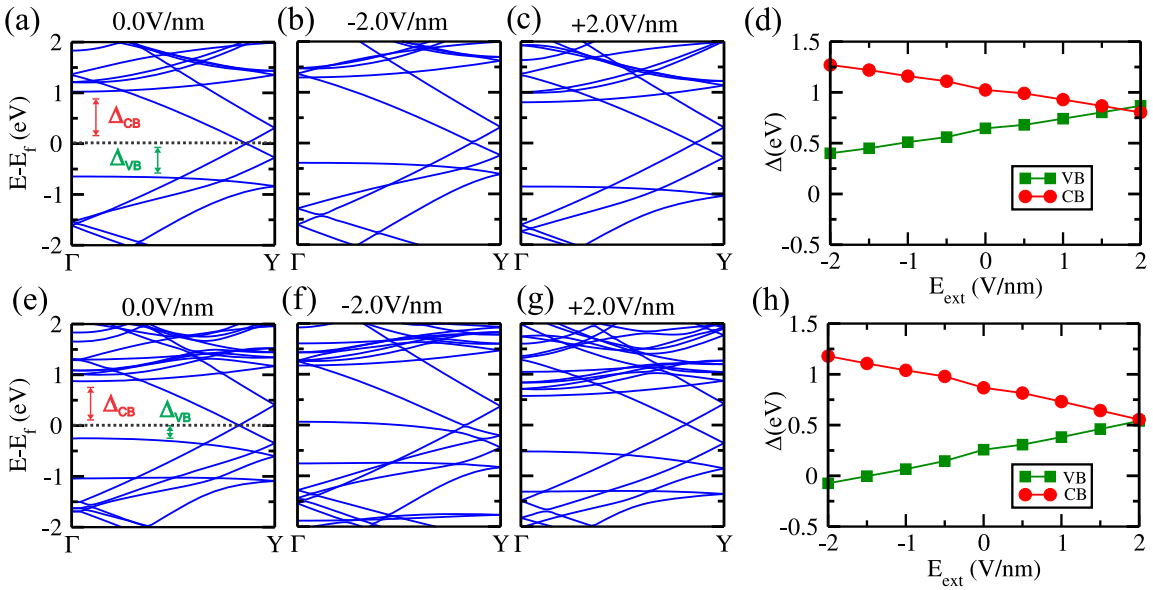

FIG. 4 (color online). Evolution of the band structure as a function of the external electric field for (a)–(c) single-layer phosphorene and (e)–(g) bilayer phosphorene. Evolution of the band edges, as a function of the field relative to the graphene Dirac point, for (d) single-layer phosphorene and (h) bilayer phosphorene. The field is applied along the z direction defined in Fig. 1 (perpendicular to the layers). The Fermi level of the systems were set to zero and VB (CB) represents top (bottom) of the valence (conduction) band.

between the layers. For the single layer, we obtained a SBH of 0.64 eV, whereas for the bilayer it is 0.26 eV. In both systems, the conduction will be through holes. Moreover, if we can make this value negative, we can induce an Ohmic contact. To this end, we applied a perpendicular electric field to both systems in order to tune their electronic structures.

In Fig. 4, we show the evolution of the band structure and band edges of single-layer (1P) and bilayer (2P) phosphorene on top of graphene, subjected to an external electric field (perpendicular to the layers). As can be seen from the band structures in Figs. 4(b) and 4(c) for the 1P system and 4(f) and 4(g) for the 2P system, application of a negative electric field makes the valence band of phosphorene closer to the Dirac cone of graphene, whereas for a positive field the conduction band gets closer. In Figs. 4(d) and 4(h) we show the evolution of the band edges, Δ_{CB} and Δ_{VB} as functions of the external electric field. Δ_{CB} and Δ_{VB} are defined as the energy differences between the conduction band minimum (CB) and valence band maximum (VB) of phosphorene relative to the Dirac point of graphene, as shown in Figs. 4(a) and 4(e). Without any applied field, as already pointed out, for both systems the valence band is closer to the Dirac point, leading to a p-type Schottky barrier. For positive values of the field, and for the single-layer case, it is possible to change this Schottky barrier from p-type to n-type for fields larger than ≈ 1.8 V/nm, whereas for the bilayer case, the Schottky barrier character remains p-type up to 2.0 V/nm, even though our results in Fig. 4(h), indicate that for larger electric fields the character will also change to n-type, like the monolayer. For negative values of the field, for both systems, the SBH always remains p-type, decreasing its value linearly with the field. An important point to note is that for the bilayer system the Dirac cone is energetically below the valence band maximum of phosphorene for negative fields smaller than ≈ -1.8 V/nm, turning this contact into an Ohmic one.

If we consider the 2P system as the gate region of a device, and the graphene layer as the gate electrode, we can use the external electric field to induce charge carriers in the channel (phosphorene). This technique has already been used in metal/h-BN/graphene [47] and graphene/MoS_2 [48]. In our results, we see that for external negative fields smaller than -1.8 V/nm, we can induce an electron transfer from the phosphorene system to the graphene layer, inducing a p-type doping of the phosphorene channel (see the Supplemental Material, Fig. S3 [44]). For fields bigger than -1.8 V/nm, there is no charge transfer and consequently no doping.

In conclusion, the structural and electronic properties of single-layer and bilayer phosphorene with graphene were studied by means of density functional theory calculations. We show that both the properties of graphene and phosphorene are preserved upon their contact. We also show that it is possible to tune the position of the band structure of phosphorene relative to that of graphene through the application of an external electric field perpendicular to the system. This allows significant control of the Schottky barrier height as well as the doping of phosphorene. In particular, for the bilayer system, it is possible to even move the system into an Ohmic contact. All of these features are quite fundamental for the design of new devices based on van der Waals heterostructures.

This work was supported by the Brazilian agencies FAPESP and CNPq. We would like to acknowledge computing time provided on the Blue Gene/P supercomputer supported by the Research Computing Support Group (Rice University) and Laboratório de Computação Científica Avançada (Universidade de São Paulo).

*padilha@if.usp.br
†fazzio@if.usp.br
‡jose.roque@lnls.br

[1] J. M. Hamm and O. Hess, Science **340**, 1298 (2013).
[2] S. Z. Butler *et al.*, ACS Nano **7**, 2898 (2013).
[3] K. J. Koski and Y. Cui, ACS Nano **7**, 3739 (2013).
[4] K. S. Novoselov, A. K. Geim, S. V. Morozov, D. Jiang, Y. Zhang, S. V. Dubonos, I. V. Grigorieva, and A. A. Firsov, Science **306**, 666 (2004).
[5] A. K. Geim and K. S. Novoselov, Nat. Mater. **6**, 183 (2007).
[6] F. Schwierz, Nat. Nanotechnol. **5**, 487 (2010).
[7] Y.-M. Lin, C. Dimitrakopoulos, K. A. Jenkins, D. B. Farmer, H.-Y. Chiu, A. Grill, and Ph. Avouris, Science **327**, 662 (2010).
[8] P. Miró, M. Audiffred, and T. Heine, Chem. Soc. Rev. **43**, 6537 (2014).
[9] Q. H. Wang, K. Kalantar-Zadeh, A. Kis, J. N. Coleman, and M. S. Strano, Nat. Nanotechnol. **7**, 699 (2012).
[10] B. Radisavljevic, A. Radenovic, J. Brivio, V. Giacometti, and A. Kis, Nat. Nanotechnol. **6**, 147 (2011).
[11] L. Li, Y. Yu, G. J. Ye, Q. Ge, X. Ou, H. Wu, D. Feng, X. H. Chen, and Y. Zhang, Nat. Nanotechnol. **9**, 372 (2014).
[12] H. O. H. Churchill and P. Jarillo-Herrero, Nat. Nanotechnol. **9**, 330 (2014).
[13] H. Liu, A. T. Neal, Z. Zhu, Z. Luo, X. Xu, D. Tomanék, and P. D. Ye, ACS Nano **8**, 4033 (2014).
[14] A. S. Rodin, A. Carvalho, and A. H. Castro Neto, Phys. Rev. Lett. **112**, 176801 (2014).
[15] J. Guan, Z. Zhu, and D. Tomanék, Phys. Rev. Lett. **113**, 046804 (2014).
[16] K. Lam, Z. Dong, and J. Guo, IEEE Electron Device Lett. **35**, 963 (2014).
[17] M. Buscema, D. J. Groenendijk, S. I. Blanter, G. A. Steele, H. S. J. van der Zant, and A. Castellanos-Gomez, Nano Lett. **14**, 3347 (2014).
[18] M. Engel, M. Steiner, and Ph. Avouris Nano Lett.. **14**, 6414 (2014).
[19] A. K. Geim and I. V. Grigorieva, Nature (London) **499**, 419 (2013).
[20] G. Gao, W. Gao, E. Cannuccia, J. Taha-Tijerina, L. Balicas, A. Mathkar, T. N. Narayanan, Z. Liu, B. K. Gupta, J. Peng, Y. Yin, A. Rubio, and P. M. Ajayan, Nano Lett. **12**, 3518 (2012).
[21] C.-J. Shih, Q. H. Wang, Y. Son, Z. Jin, D. Blankschtein, and M. S. Strano, ACS Nano **8**, 5790 (2014).
[22] Y. Deng, Z. Luo, N. J. Conrad, H. Liu, Y. Gong, S. Najmaei, P. M. Ajayan, J. Lou, X. Xu, and P. D. Ye, ACS Nano **8**, 8292 (2014).
[23] H. Wang, L. Yu, Y.-H. Lee, Y. Shi, A. Hsu, M. L. Chin, L.-J. Li, M. Dubey, J. Kong, and T. Palacios, Nano Lett. **12**, 4674 (2012).
[24] M. Bernardi, M. Palummo, and J. C. Grossman, Nano Lett. **13**, 3664 (2013).
[25] M. M. Furchi, A. Pospischil, F. Libisch, J. Burgdörfer, and T. Mueller, Nano Lett. **14**, 4785 (2014).
[26] T. Roy, M. Tosun, J. S. Kang, A. B. Sachid, S. B. Desai, M. Hettick, C. C. Hu, and A. J. Javey, ACS Nano **8**, 6259 (2014).
[27] L. Yu, Y.-H. Lee, X. Ling, E. J. G. Santos, Y. C. Shin, Y. Lin, M. Dubey, E. Kaxiras, J. Kong, H. Wang, and T. Palacios, Nano Lett. **14**, 3055 (2014).
[28] K. Gong, L. Zhang, W. Ji, and H. Guo, Phys. Rev. B **90**, 125441 (2014).
[29] G. Kresse and J. Furthmüller, Phys. Rev. B **54**, 11169 (1996).
[30] G. Kresse and J. Furthmüller, Comput. Mater. Sci. **6**, 15 (1996).
[31] J. P. Perdew, K. Burke, and M. Ernzerhof, Phys. Rev. Lett. **77**, 3865 (1996).
[32] P. E. Blöchl, Phys. Rev. B **50**, 17953 (1994).
[33] J. Klimeš, D. R. Bowler, and A. Michaelides, J. Phys. Condens. Matter **22**, 022201 (2010).
[34] J. Klimeš, D. R. Bowler, and A. Michaelides, Phys. Rev. B **83**, 195131 (2011).
[35] J. Qiao, X. Kong, Z.-X. Hu, F. Yang, and W. Ji, Nat. Commun. **5**, 4475 (2014).
[36] H. Guo, N. Lu, J. Dai, X. Wu, and X. C. Zeng, J. Phys. Chem. C **118**, 14051 (2014).
[37] To benchmark our structural calculation, we have determined for the black phosphorus bulk the lattice parameters with optB88-vdw, where for the lattice constants we obtain $a = 4.41$ Å, $b = 3.31$ Å, and $c = 10.44$ Å, in good agreement with the experimental values ($a = 4.38$ Å, $b = 3.31$ Å, and $c = 10.48$ Å).
[38] J. Heyd, G. E. Scuseria, and M. Ernzerhof, J. Chem. Phys. **118**, 8207 (2003).
[39] J. Heyd, G. E. Scuseria, and M. Ernzerhof, J. Chem. Phys. **124**, 219906 (2006).
[40] With HSE06, we obtained for the band gap of the bulk black phosphorus around 0.37 eV—that is in agreement with the experimental values [41–43].
[41] R. W. Keyes, Phys. Rev. **92**, 580 (1953).
[42] Y. Maruyama, S. Suzuki, K. Kobayashi, and S. Tanuma, Physica (Amsterdam) **105**, 99 (1981).
[43] Y. Akahama, S. Endo, and S.-I. Narita, J. Phys. Soc. Jpn. **52**, 2148 (1983).
[44] See Supplemental Material at http://link.aps.org/supplemental/10.1103/PhysRevLett.114.066803 for band structures of single-layer phosphorene over graphene for several displacements δ_x and δ_y; band structure and band edges for the single-layer phosphorene over graphene in the graphene lattice constant; and charges as a function of the electric field for the bilayer phosphorene on top of graphene.
[45] G. Graziano, J. Klimeš, F. Fernandez-Alonso, and A. Michaelides, J. Phys. Condens. Matter **24**, 424216 (2012).
[46] P. A. Khomyakov, G. Giovannetti, P. C. Rusu, G. Brocks, J. van den Brink, and P. J. Kelly, Phys. Rev. B **79**, 195425 (2009).
[47] M. Bokdam, P. A. Khomyakov, G. Brocks, Z. Zhong, and P. J. Kelly, Nano Lett. **11**, 4631 (2011).
[48] B. Sachs, L. Britnell, T. O. Wehling, A. Eckmann, R. Jalil, B. D. Belle, A. I. Lichtenstein, M. I. Katsnelson, and K. S. Novoselov, Appl. Phys. Lett. **103**, 251607 (2013).